Journal of Molecular Graphics and Modelling 27 (2009) 712–722

Contents lists available at ScienceDirect

Journal of Molecular Graphics and Modelling

journal homepage: www.elsevier.com/locate/JMGM

Inside the Hsp90 inhibitors binding mode through induced fit docking

Antonino Lauria *, Mario Ippolito, Anna Maria Almerico

Dipartimento Farmacochimico, Tossicologico e Biologico, Università di Palermo, Via Archirafi 32, 90123 Palermo, Italy

ARTICLE INFO

Article history:
Received 2 July 2008
Received in revised form 1 October 2008
Accepted 3 November 2008
Available online 8 November 2008

Keywords:
Heat shock protein
Geldanamicyn
Radicicol
Induced fit
Molecular docking

ABSTRACT

During the last few decades, the development of new anticancer strategies had to face the instability of many tumors, occurring when the genetic plasticity of cells produces new drug-resistant cancers. It has been shown that a chaperone protein, heat shock protein 90 (Hsp90), is one of the fundamental factors involved in the cell response to stresses, and its role in many biochemical pathways has been demonstrated. Thus, the inhibition of Hsp90 represents a new target of antitumor therapy, since it may influence many specific signaling pathways.

The natural antibiotic Geldanamycin is the first Hsp90 inhibitor that has been identified. Nevertheless, more potent and water-soluble small molecules are currently in development, and many X-ray crystallographic structures of Hsp90-inhibitor complexes are available for drug discovery purposes. Here we used the complexes of Hsp90 with eight different ligands, belonging to several chemical classes, to perform molecular docking experiments, using a novel technique called induced fit. Through this approach, it was possible to take into account the flexibility of the residues in the active site and to maintain a high level of precision in docking algorithms.

The results allowed to identify several conserved residues involved in the interaction between Hsp90 and its inhibitor. Moreover, the exposition of the active site to solvent allows many water molecules to insert within the complex, providing additional hydrogen and polar interactions. Our models also provided template structures for further experiments and reproduces with a good degree of reliability, the conformations of the inhibitors as observed in experimental structures.

1. Introduction

The genetic instability of many tumor diseases represents one of the most difficult obstacles to overcome. In the last decades, promising efforts have been made in the improvement of chemotherapy regimens through the development of novel and more selective therapeutic agents. Despite the specific inhibition of individual proteins or signaling pathways, this approach becomes unsuccessful when the genetic plasticity of cancer cells produces drug-resistant tumor lines. In fact, cancer cells are very efficient in adapting their genetic apparatus to the noxious environment which represents a source of stresses for the cell cycle. Thus, hormone-dependent tumors become hormone-independent; similarly the hypoxia, occurring when the tumor growth outstrips the accompanying angiogenesis, induces a multi-factorial response geared to survive such an environment. Moreover, the massive exposure to a previous successful chemotherapy scheme activates multiple overlapping signal pathways, with the global effect to protect the cancer cells from further harm. Therefore, it is clear why the understanding of molecular mechanisms underlying the multi-factorial stress response is of great importance in the drug design phase of cancer therapy.

From early 1990s, several groups [1–4] reported that the cells respond to stresses by increasing the synthesis of a number of molecular chaperones known as heat shock proteins (or Hsp, because they first were observed in cells exposed to high temperatures). These proteins play an "housekeeping" role in stress response, since they assist general protein folding and prevent non-functional side reaction, such as the non-specific aggregation of misfolded or unfolded proteins. In particular, heat shock protein 90 (Hsp90) emerged as being of prime importance for the survival of cancer cells exposed to stresses, influencing the activity and stability of many proteins that function as key regulators in cellular growth, differentiation and apoptotic pathways. Its fundamental role is suggested by the observation of Hsp90 expression at 2–10-fold higher levels in tumor cells, compared with their normal counterparts [5]. Moreover, the number of proteins and pathways in which Hsp90 assumes a

* Corresponding author. Tel.: +39 0916161606; fax: +39 0916169999.
E-mail address: lauria@unipa.it (A. Lauria).

1093-3263/$ – see front matter © 2008 Elsevier Inc. All rights reserved.
doi:10.1016/j.jmgm.2008.11.004

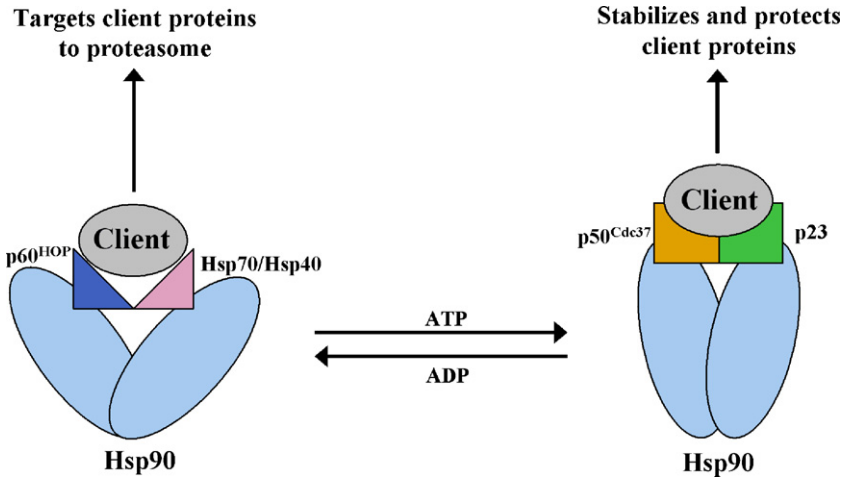

Fig. 1. ATP-dependent cycle of the HSP90 super-chaperone machine.

regulatory role still continues to grow, including several cancer mutated or overexpressed factors such as p53, Akt kinase, Raf-1 kinase, Bcr-Abl kinase, ErbB2 transmembrane kinase, cyclin-dependent kinases Cdk4 and Cdk6, the cell-cycle-associated kinase Wee1, certain basic helix–loop–helix transcription factors including Hypoxia-inducible factor 1α (HIF-1α) and estrogen and androgen steroid receptors [6,7].

The chaperone mechanism of Hsp90 has been proposed [8,9] as consisting of the formation of a "super-chaperone machine" constituted by a multi-factor complex. ATP binds the N-terminal pocket and triggers a conformational change among at least two main conformations (Fig. 1).

The Hsp90 client protein first associates with the Hsp70/Hsp40 chaperone complex, and the resulting assemblage is further linked to Hsp90 through the $p60^{HOP}$ Hsp90/70 interacting protein. At this point, when the client protein is loaded on Hsp90, the replacement of ADP with ATP alters its conformation, releasing $p60^{HOP}$ and Hsp70/Hsp40 chaperone complex and recruiting another set of co-chaperones, including $p50^{Cdc37}$ and p23. This association stabilizes client proteins and temporarily holds them in a state that can bind ligands or can be translocated into the nucleus. If a client protein fails to receive its stimulus (ligand, phosphorilation and translocation) while the complex is in the receptive conformation, the cycle will reverse. After ATP hydrolysis Hsp90 is altered, releasing the co-chaperones that associate with the ATP-bound conformation and restoring the ADP-complex. In this state the client protein can be unloaded from the whole complex and addressed to the proteasome-dependent degradation pathway. However, the mechanism by which the client protein is targeted for degradation is not fully known, and may depend on the frequency at which the ADP-complex is capable of recruiting specific ubiquinating and proteasome-interacting factors.

Originally discovered as a naturally occurring antitumor antibiotic [10], Geldanamycin (GA, Fig. 2a) is the first Hsp90 inhibitor that has been identified. Although GA displays high potency in cytotoxicity assays, it also showed hepatotoxicity in preclinical trials [11], probably because of the presence of the quinone moiety and/or the high reactivity of the 17-methoxy group towards nucleophiles. Thus, analogs with 17-alkylamino groups, with a reduced hepatotoxicity, have been synthesized. Although one of these compounds, 17-allylamino-17-demethoxygeldanamicyn (17AAG, Fig. 2b) showed antitumor activity in Phase I studies, its water insolubility made it difficult to formulate. Finally the preclinical evaluation of 17-desmethoxy-17-N,N-dimethylaminoethylaminogeldanamicyn (17DMAG, Fig. 2c) demonstrated it to be more potent and more water soluble than 17AAG and provided an excellent bioavailability [12]. To date, the main target of Hsp90 inhibitors research is the design of small inhibitors which can be delivered orally. Even though many structural classes of Hsp90 inhibitors have been synthesized, only

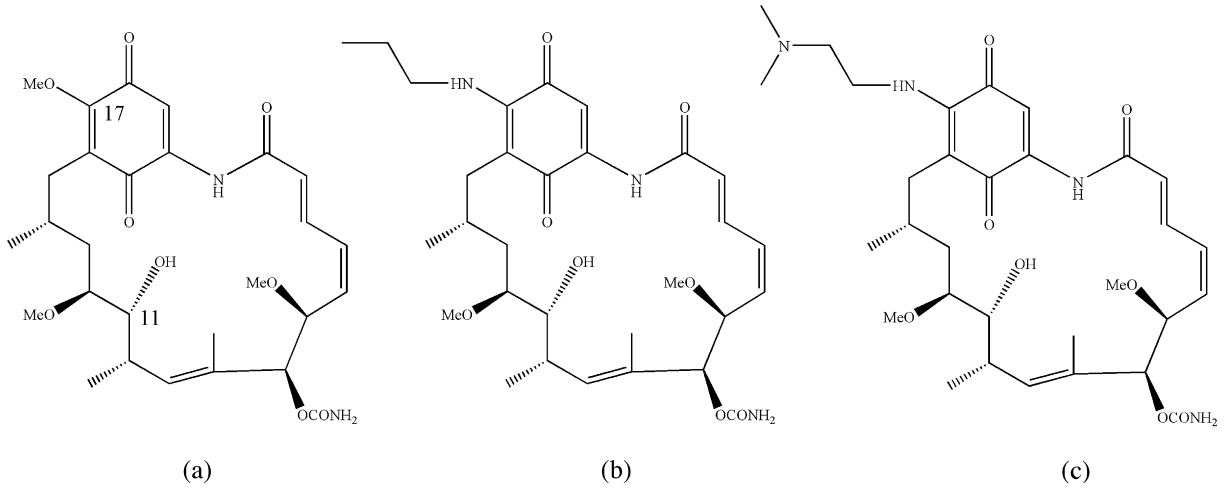

Fig. 2. (a) Geldanamicyn, (b) 17AAG and (c) 17DMAG.

SNX-5422 (developed by Serenex™) was recently announced to have entered Phase Two clinical trials for oral administration [13]. However, many structural classes have been demonstrated to be Hsp90 agonist [14,15]. X-ray crystallography showed that each inhibitor occupies the ATP binding cavity placed in the N-terminal domain of Hsp90 and interacts with many residues of the active site, both directly and through the insertion of water molecules.

Since several X-ray complexes between Hsp90 and inhibitors, belonging to very different classes, are freely available in the RCSB protein data bank (PDB) [16], we performed a comparative analysis of the different Hsp90/ligand complexes available in the PDB, with the aim of investigating the binding mode of each structural class and giving an overall comparative view of all the interactions occurring in each complex. In order to achieve this goal, we carried out molecular docking experiments using a novel procedure called induced fit docking (IFD) [17] which takes into account the receptor flexibility and at the same time gives insights into the specific protein/ligand interactions.

2. Materials and methods

2.1. Selection of the derivatives

The selection of all the classes of Hsp90 inhibitors, for which X-ray crystallographic structures are available, was performed using the Binding Database [18], a public web-accessible database of measured binding affinities focused on the interaction between drug–target proteins and small molecules. All the entries were classified according to their molecular core structure and to the availability of the receptor/drug complex PDB structure. This allowed us to identify several of Hsp90 agonists providing the lowest IC_{50} value for each structural class (Figs. 2a, 2c and 3): GA (PDB code: 1YET) [19], Radicicol (PDB code: 1BGQ) [20], 2,5-dichloro-N-[4-hydroxy-3-(2-hydroxy-1-naphthyl)phenyl] (naphtol 11, PDB code: 2BZ5) [21], 3-(5-chloro-2,4-dihydroxyphenyl)-N-ethyl-4-(4-methoxyphenyl)-1H-pyrazole-5-carboxamide (VER49009, PDB code: 2BSM) [22,23], 8-(2-chloro-3,4,5-trimethoxybenzyl)-9-pent-4-yn-1-yl-9H-purin-6-amine (purine 8, PDB code: 1UYF) [24] and 4-isopropyl-6-{3-[4-(morpholin-4-ylmethyl)phenyl]-N-ethyl-isoxazol-4-yl-5-carboxamide}benzene-1,3-diol (isoxazole 40f, PDB code: 2VCI) [25]. In addition, the complex containing the natural agonist of Hsp90, ATP, was also investigated (PDB code: 1AM1) [26].

2.2. Hsp90 site mapping

Firstly, the active site from each PDB complex was investigated using SiteMap program [27]. This software generates information on the binding site's characteristics using novel search and analytical facilities: a SiteMap calculation begins with an initial search step which identifies or characterizes, through the use of a grid points, one or more regions on the protein surface that may be suitable for binding of ligands to the receptor. Then contour maps are generated, producing hydrophobic and hydrophilic maps. The hydrophilic maps are further divided into donor, acceptor, and metal binding regions. The evaluation stage, which concludes the calculation, assesses each site by calculating various properties: Number of site points, a measure of the site size; exposure/enclosure, two properties providing different measures of how available is the site to the solvent; contact, which measures how strongly the average site point interacts with the surrounding receptor via van der Waals non-bonded interactions; donor/acceptor character, a property related to the sizes and intensities of H-donor and H-acceptor regions; SiteScore, an overall property based on previous properties, constructed and calibrated so that the average SiteScore for a promising binding site is 1.0.

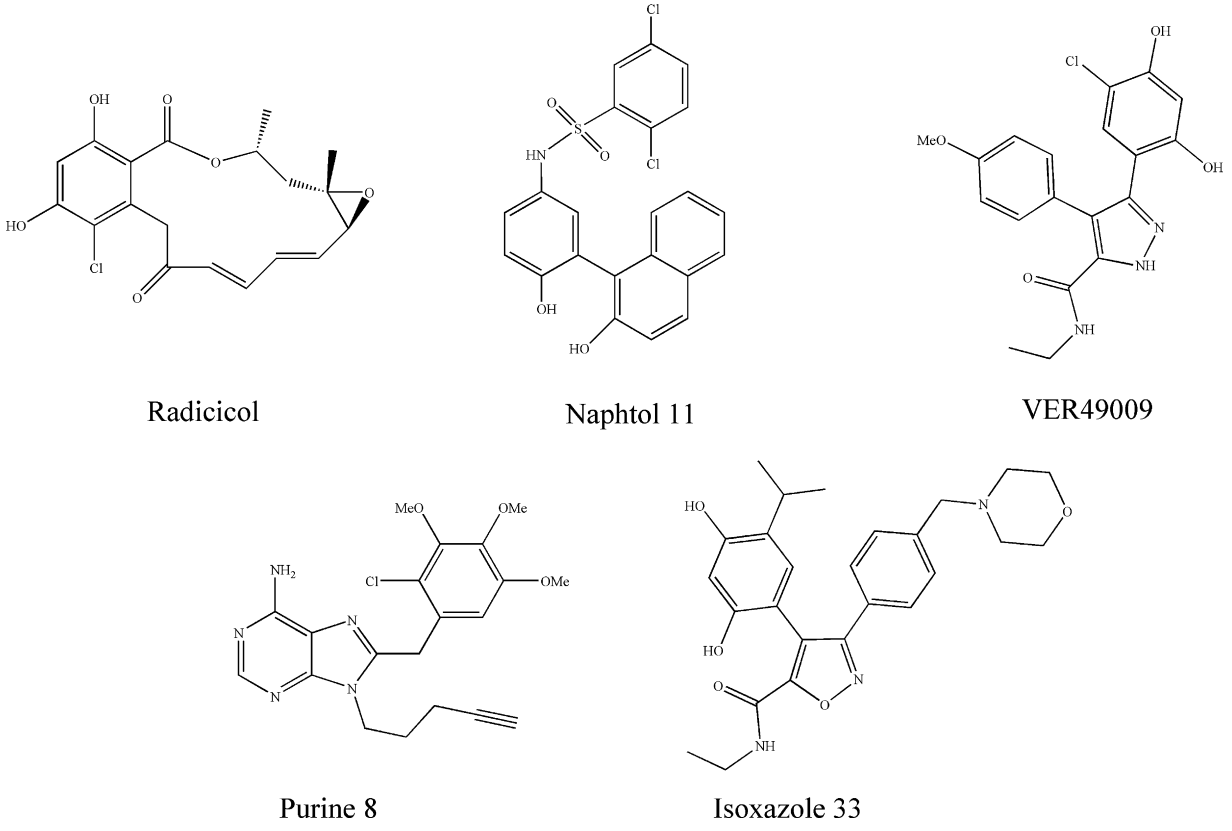

Fig. 3. Derivatives involved in this study.

2.3. Induced fit docking

The important role of molecular docking in the study of drug–target interactions has been universally recognized in the last 20 years [28,29]; from its first application in early 1980s, this technique has become a fundamental tool in the field of drug discovery and lead optimization. Over the years, several important steps have been made toward the improvement of accuracy predictions. In particular, the problem of efficiently handling the receptor flexibility is still considered one of the hardest challenges; even though the target macromolecule can be considered as a rigid body, it has been shown [30] that large localized rearrangements of the protein surface frequently occur, especially in the ligand binding domains and in large flexible amino acid chains. Nevertheless, the implementation of full conformational flexibility during a docking experiment results infeasible, because of the great amount of time and computational resources requested by these calculations. Many efforts have been made in order to overcome this obstacle [31], and the resulting approaches can be classified in two broad classes: the methods that account for receptor reconstruction by combining multiple conformations of target macromolecule from experiments or simulations (ensemble-docking approach), and the methods that sample receptor flexibility during the docking simulation (induced-fit approach).

The first examples of ensemble-docking approaches involved the use of a composite grid incorporating multiple NMR or crystallographic structures of protein/ligand complexes [32], and gave encouraging results, even if it did not take into account the combinatorial nature of the conformations used. Alternative simulations [33] involved the use of many crystal structure of complexed inhibitors, superimposing by their most stable regions, with the aim to create a composite map of the binding site. Molecular Dynamics, Monte Carlo and rotamer libraries methods [34,35] have also been tried with the aim of introducing at least partially flexibility in the receptor macromolecule. The global advantage of such methodologies is their effectiveness in finding new lead candidates that would have been missed in rigid receptor docking or reproducing complex conformations of known compounds. The induced-fit approach appears more promising, since it allows the complete exploration of the conformational space of the protein, by covering a larger set of receptor orientations. Nevertheless, this methodology appears to be more time consuming, because protein flexibility requires the sampling of a large number of degrees of freedom in the simulation.

To explore the binding properties of each Hsp90 inhibitor, the induced fit docking protocol, developed by Schrödinger Inc. [17], was employed. This approach combines in an iterative fashion the ligand docking techniques with those for modeling receptor conformational changes. The Glide docking program [36] is used for ligand flexibility, while the refinement module in prime program [37] is used to account for receptor flexibility: the side chain degrees of freedom are mainly sampled, while minor backbone movements are allowed through minimization. The major feature of the side chain prediction algorithm is the sampling performed in a dihedral angle space: in fact, although the algorithm uses the same type of force field-based energy functions used in molecular dynamics (MD), the small moves are replaced with large moves in dihedral angle space. Moreover, other important features include the rapid elimination of conformations that involve steric clashes, the efficient minimization algorithm (multi-scale Truncated Newton), the use of rotamer libraries to sample only energetically reasonable side chains conformations. All these features are coupled in an iterative process, depicted in Fig. 4: the strategy is to dock first ligands into a rigid receptor using a softened energy function such that steric clashes do not prevent

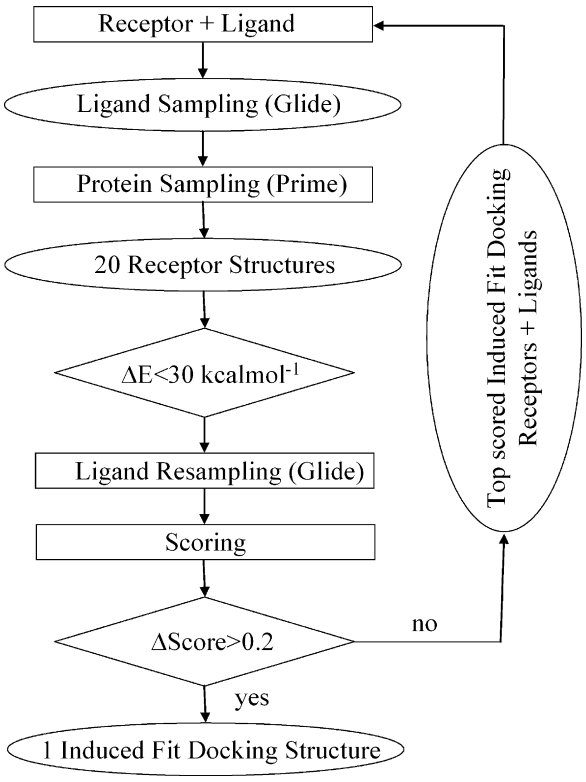

Fig. 4. Induced fit docking flowchart.

at least one pose from assuming a conformation close to the correct one (ligand sampling step); further, the receptor degrees of freedom are sampled, and a global ligand/receptor energy minimization is performed for many ligand poses which attempts to identify low free-energy conformations of the whole complex (protein sampling step). A second round of ligand docking is then performed on the refined protein structures, using a hard potential function to sample ligand conformational space within the refined protein environment (ligand resampling step). Finally a composite score function is applied to rank the complexes, accounting for the receptor/ligand interaction energy as well as strain and solvation energies (scoring step). The challenge of the initial ligand sampling step is to generate at least one reasonably docked pose for the ligand (independent from the score it receives), because without a plausible initial guess for the ligand pose, any attempt to predict reorganization of the protein structure is unlikely to succeed in the context of a limited allotment of CPU time. The main goal of the protein sampling step is to predict the low energy receptor conformation for a correct ligand pose, starting from the plausible initial guess previously generated. The ligand resampling step is focused on the generation of low energy conformations when presented with the correct receptor conformation.

The composite score used for final ranking of compounds is given by GlideScore + 0.05 × PrimeEnergy This definition implies that in most cases GlideScore term is dominant; however, the small contribution of PrimeEnergy score is sufficient to eliminate predicted protein structures for which the energy gap is large enough to overcome the energy noise introduced by minor steric clashes. In fact, if the gap in composite scores between top ranked structures is below 0.2, indicating isoenergetic solutions, the entire IFD protocol is repeated for the top ranked solutions using the results from the first IFD as input for a further cycle.

Before the docking run, each complex was prepared by adding hydrogens and charges, in particular setting the ionization state of

charged residues to physiological conditions. Moreover, the water molecules originally crystallized within the protein were selectively deleted, except for those included in a 5 Å radius sphere centered on the ligand. The induced fit parameters were set as following: during the initial Glide docking a van der Waals radius scaling of 0.50 Å was kept for both ligand and receptor atoms, and the top 20 poses were recorded. For the Prime refinement step, all the residues within 5 Å from the active site were kept free to move, and the side chains were further minimized. Finally, in the Glide redocking step, all the conformations within 30 kcal mol^{-1} from the best one were accepted; as available in Glide [36], the accuracy level was set to the extra-precision mode (XP), combining a powerful sampling protocol with the use of a custom scoring function to identify ligand poses expected to have unfavourable energies, designed as a refinement tool for use only on good ligand poses.

Finally, as the results from each induced fit docking run were examined, the quality of each model was further validated through the Ramachandran Plot generated using the Rampage server [38], which showed a low fraction of all residues (<2.8%) falling outside the favorable regions [see Supporting material]. For the selection of best poses a double criteria was used, taking into account both energetic parameters (IFD Score) and proximity to the original structure crystallized with Hsp90: a common pattern was observed, sine the poses providing the best IFD Score values also provided lowest RMSD.

3. Results and discussion

As the main aim of our work is to investigate the different binding modes of N-terminal Hsp90 agonists, by taking into account the structural flexibility of the protein, we first evaluated the active site of each crystallographic complex in terms of shape, steric, and electronic properties (Table 1). From the calculated values it emerges that all complexes have a good SiteScore (with an average value of 0.99), which qualifies each pocket as tight drug binding sites. Moreover, the value of enclosure score (>0.70) reveals that a high degree of burial is a common characteristic of all the complexes investigated. From the contact scores it also emerges that the strength of van der Waals contacts with the receptor is an important feature of each active site; the ratio between H-donor and H-acceptor character of the grid maps is quite balanced, indicating that both properties are desirable in a well-structured ligand for a tight receptor binding. However the size of each active site is variable, according to the ligand originally crystallized into the pocket.

The inspection of the binding cavity site (Fig. 5) is totally consistent with the previous observations, showing that the binding cavity is partially buried into the protein structure and at the same time has a plethora of H-bond donor and acceptor sites on its solvent-exposed side. In this case the overlap between the crystallized ligand (ATP) and each area is remarkable, with the aromatic purine ring and the sugar carbon skeleton occupying the hydrophobic area of the site, and the heteroatoms containing substituents taking contacts with the H-bond favourable areas.

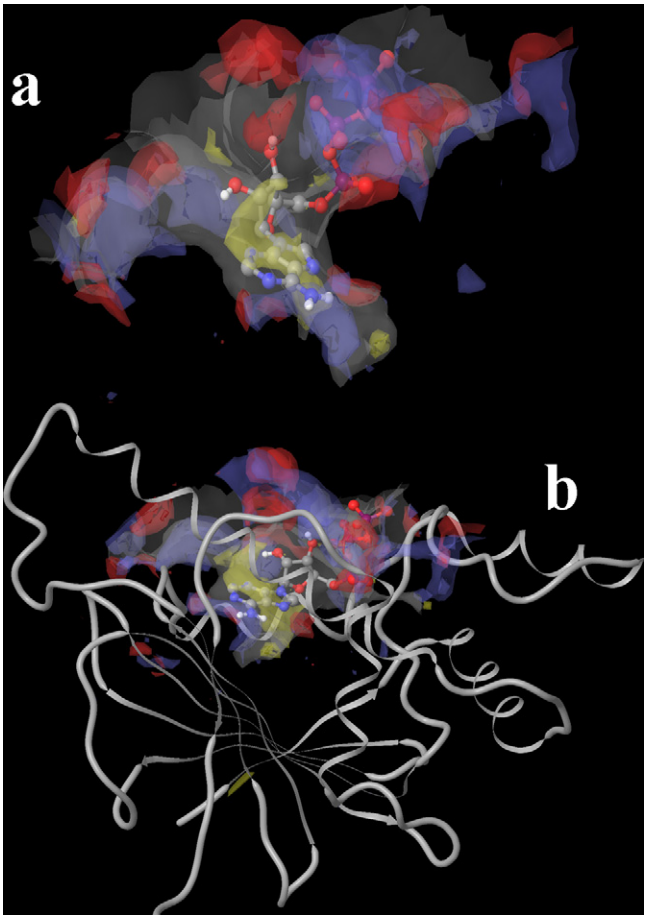

Fig. 5. (a) Active site of Hsp90 (ATP complex) and (b) active site of Hsp90 within the whole protein. Grey: vdW surface. Yellow: hydrophobic map. Red: H-donors map. Blue: H-acceptors map.

Table 1
SiteMap results for the investigated crystallized complexes # Site points: number of site points; exposure/enclosure: properties measuring the degree of opening of active site to the solvent; contact: measure of site point interaction via vdW contacts; Don/Acc: property related to the sizes and intensities of H-bond donor and acceptor regions; SiteScore, an overall score based on previous properties.

PDB ID code	# Site points	Exposure	Enclosure	Contact	Don/Acc	SiteScore
1AM1	112	0.59	0.73	0.93	0.94	0.96
1BGQ	107	0.65	0.72	0.85	0.90	0.94
1UYF	233	0.48	0.78	1.01	1.00	1.07
1YET	117	0.66	0.71	0.82	0.97	0.92
2BSM	126	0.48	0.77	1.01	1.29	1.01
2BZ5	139	0.49	0.79	0.98	1.14	1.02
2VCI	135	0.46	0.76	0.99	1.45	1.01
Average	138	0.54	0.75	0.94	1.10	0.99

With the aim of investigating dynamic behavior of the active site during the binding of ligands belonging to different classes, we performed induced fit docking experiments on eight derivatives incorporating different core structures, using the crystallized complexes available in the protein data bank, and analyzing the similarities between the docked poses and the original structures.

The first structure to be examined was the 1AM1, in which Hsp90 is complexed with its natural ligand, ATP. According to previous results [20,24] the ATP binding pocket is bound by helices comprised between residues 28–50, 85–94 and 81–85, with a base formed by residues Ile77, Asp79, Val136, Ser138 Thr171 and Ile173 (Fig. 6a). The crystallized ligand makes extensive interactions with both solvent and protein; in particular, the adenine ring penertrates into the pocket and forms hydrogen interactions with Asp79, Leu34, Thr171 and Asn92. However, the ATP skeleton appears to be incomplete, since no γ-phosphate group is present: this can be explained considering the crystallization conditions involving the use of divalent cations, or a lack of resolution in correspondence of phosphate skeleton; another possible explanation involves a rapid hydrolysis of ATP followed by a conforma-

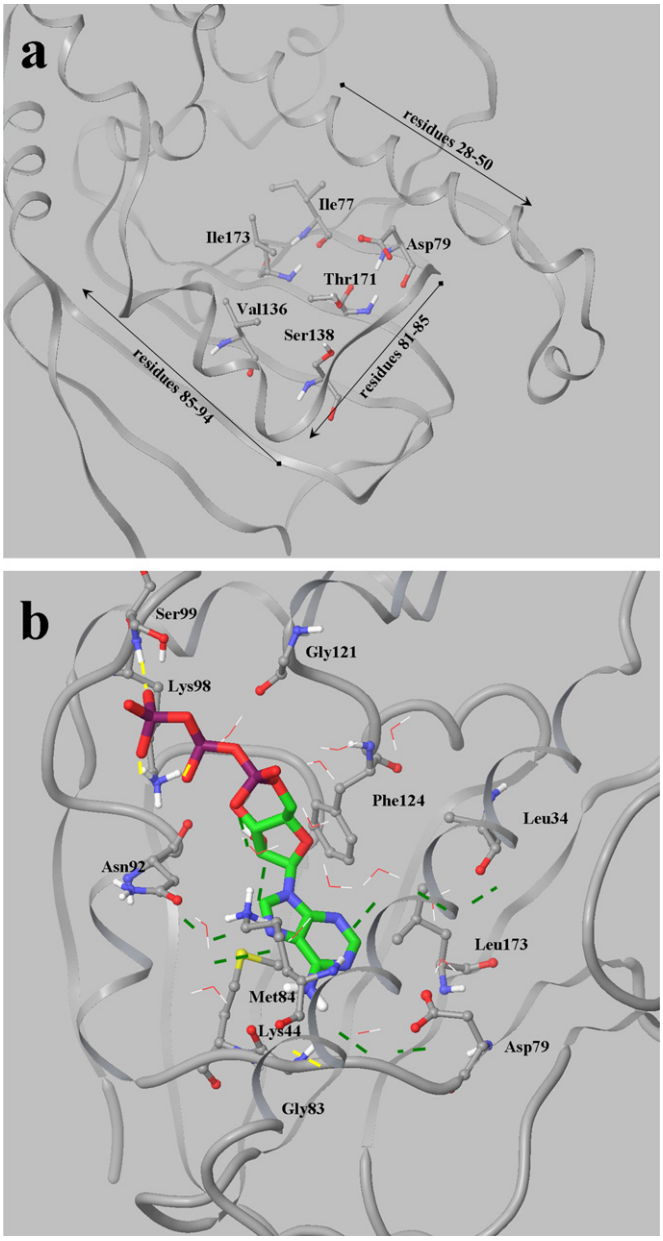

Fig. 6. (a) Binding pocket of Hsp90 and (b) model for ATP binding. Green dashes: water-mediated H-bonds; yellow dashes: direct H-bonds.

tional change resulting in a preferential binding of the diphosphate nucleotide. In our model (Fig. 6b), providing a RMSD = 3.461, the two faces of adenine experience very different conditions in terms of hydrophobicity: in fact, the bottom face of adenine is buried in a hydrophobic pocket formed by Met84, Leu173, and Phe124, which does not allow any water molecule to insert in it.

The upper side of adenine is exposed to several solvent molecules, which contribute to a network of polar and hydrogen bonding interactions with some key residues. Water-mediated H-bonds are formed between Asp79 carbonyl terminal and adenine NH_2, Leu34 and adenine N3 through two water molecules, Lys44 δ-NH_2 and adenine N7. The phosphate oxygen atoms also use intervening solvent molecules to interact with Gly121 and Asn92. Direct H-bonds occur between Gly83 and adenine NH_2 (2.49 Å), Lys98, Ser99 and phosphate oxygen atoms (1.79–1.88 Å). However, as suggested by the relatively high RMSD value, the adenine ring position appears to be rotated with respect to the crystallized ligand, even if the network of interactions is conserved. This can be explained considering the little difference between the docked ligand and the original crystallized structure. Nevertheless, an additional IFD experiment involving the binding of ADP instead of ATP (see Supplementary Material) reproduced the binding mode of the reported ligand with a RMSD = 0.540.

Further, the GA binding mode was investigated (Fig. 7). Our model (RMSD = 0.653) mainly reproduces the binding mode observed in the crystallized ligand, with minimal differences due to the different positions of some water residues. The macrocyclic ansa ring adopts a C-shaped conformation, and provides a large surface complementarity between the ligand and the binding pocket, involving several residues such as Met98, Leu107, Phe138, Leu48, Val186 and Val150, which contribute to the formation of several van der Waals interactions. The ansa carbamate nitrogen gives a hydrogen bond with Asp93 side chain carbonyl (2.01 Å) while the carbonyl oxygen atom interacts with Asp93 through a water molecule; the importance of this hydrogen bonds network is also confirmed by structure–activity studies, which demonstrated that a drastic modification of the carbamate moiety leads to a lack of activity [19]. The C11-OH group interacts with the δ-NH_2 from Lys58, while the C12 methoxy group points toward Asn106 backbone carbons. The amide oxygen forms a hydrogen bond with Phe138 backbone nitrogen (1.89 Å). The quinone ring is placed near the entrance of the binding pocket and interacts with Lys112 (2.50 Å) and Asn51 via a water molecule.

Although the ansamicyn antibiotics such as GA and its analogs have been demonstrated to be potent and selective N-terminal Hsp90 inhibitors, the similarity between GA and Radicicol (Figs. 2a and 3) has suggested that these two compounds may act in a similar fashion at molecular level. Our model for Radicicol binding mode (Fig. 8) confirms the observations that emerged from X-ray structures, which showed that the conformation is oriented in the opposite sense to GA, with the aromatic ring placed on the bottom of the ATP pocket, while the macrocycle containing the epoxide

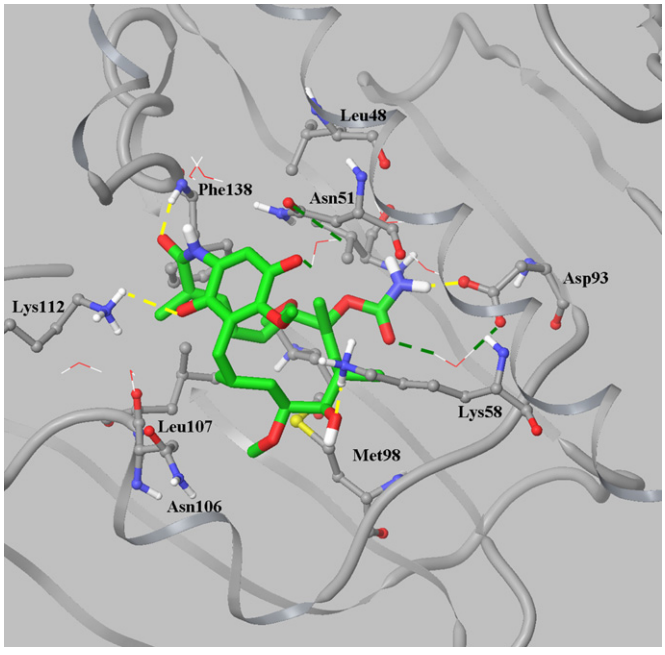

Fig. 7. Binding modes of Geldanamicyn.

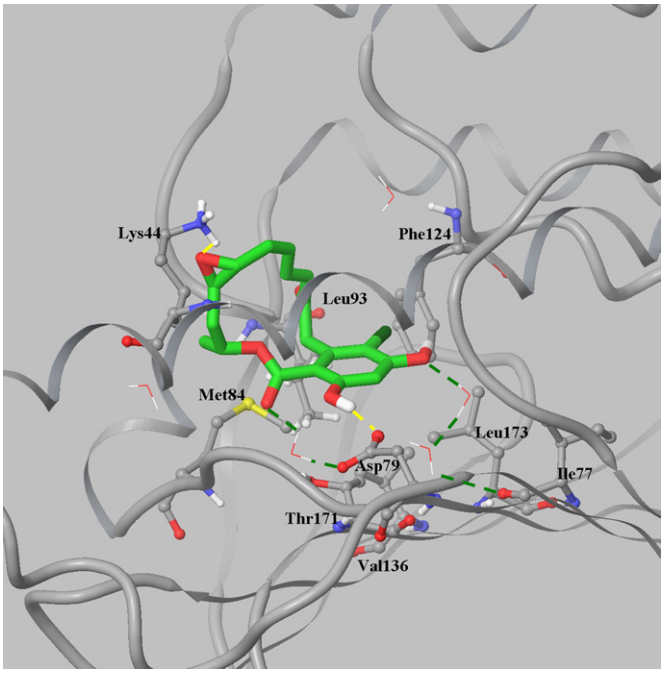

Fig. 8. Binding mode of Radicicol.

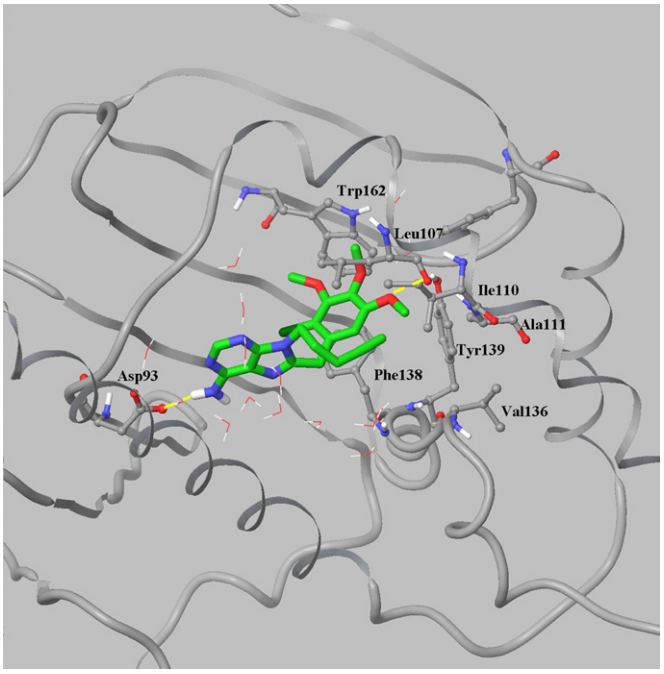

Fig. 9. Binding mode of purine 8.

moiety is direct towards the top of the pocket; the conformation obtained from IFD experiment perfectly corresponds to the crystallized structure reported (RMSD = 0.026).

The large hydrophobic complementarity existing between the ligand surface and the active site pavement (Leu173, Phe124, Leu93, Val136, Thr171 and Met84) does not allow a large number of water molecules to occupy the cavity. Hydrogen bonds are present between the resorcinol hydroxyl groups, Asp79 (1.79 Å) and Ile77 (via two water molecules). Moreover, another important hydrogen bond occurs between the epoxide oxygen atom and Lys44 δ-NH_2 (2.11 Å). However, as suggested by crystallographic studies [20], the structural data alone appear unable to provide a simple explanation of the greater affinity of Radicicol over GA, in terms of strength of interactions made in the nucleotide binding site, even if the binding mode of Radicicol involves a lower number of water molecules and does not provide significative conformational changes or does not increase ordering of protein side chains; the values of IFD Score are also unable to provide clues of this greater affinity, since GA provided a better value than Radicicol (−562.96 against −554.76).

One of the first efforts in designing non-natural Hsp90 inhibitor was oriented to the synthesis of purine-core structure compounds, which are able to mimic the natural Hsp90 substrate, ATP [39]. The binding mode of the crystallized ligand provides clues of the similarity between the binding of ATP and purine-containing derivatives, with the adenine ring placed in nearly the same position of the natural substrate of Hsp90 [24], and the methoxy groups taking contacts with Trp162 and Tyr139, as well as with the alyphatic carbons of Ala11 and Val150. Our model (Fig. 9) confirms that the position of the purine ring essentially follows the same pattern observed in the case of ATP ring, and well reproduces the binding mode observed in the case of the crystal structure (RMSD = 0.786).

In particular, the 6-NH_2 substituent of purine forms hydrogen bonds with Asp93 side chain (1.88 Å), while the nitrogen atoms of adenine ring interact with water molecules. The aryl ring appears to be stacked between the side chains of Leu107 and Phe138, forming π–π interactions with the phenyl ring of the latter. Other hydrophobic interactions involving the methoxy substituent are those with Trp162, Thr139, Phe138 and Leu107. The aliphatic substituent, instead, inserts in a hydrophobic channel formed by Val136, Ala111 and Ile110.

1-(2-Phenol)-2-naphtols, originally discovered through a virtual screening protocol [40], also demonstrated to bind Hsp90 ATP

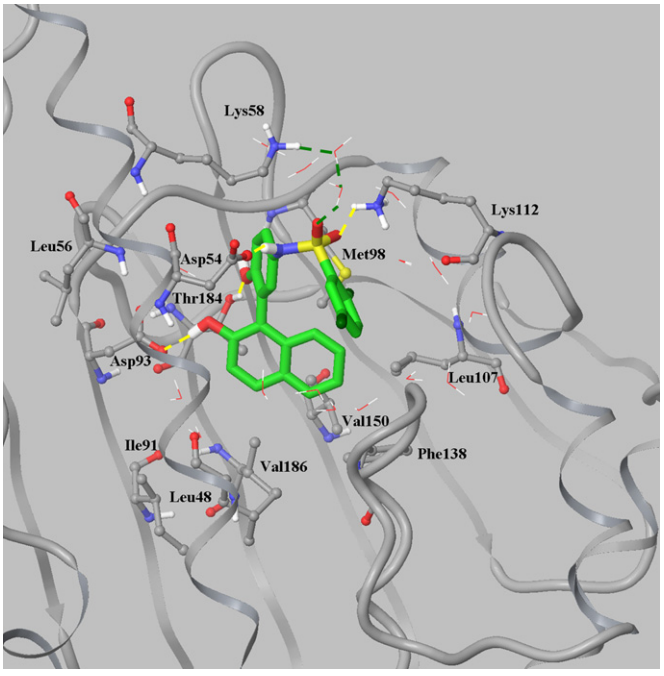

Fig. 10. Binding mode of naphtol 11.

pocket [21]. According to the reported SARs, the unsubstituted ring on the naphtol system is strictly necessary for Hsp90 binding and can be replaced only by other rings which make favourable contacts with Phe138 and maintain the position of phenol oxygen atom near Asp93 and Thr184. Moreover, the sulphonamide group does not interact with the protein, but merely acts as a linker between the phenol and benzene moieties. Our model (Fig. 10) showed that the naphtol ring is located in the same position of ATP purine ring, and inserts into a hydrophobic cavity formed by Met98, Leu107, Phe138, Leu48, Val186, and Val150. Despite the high hydrophobicity of the binding cavity, the region around residues Leu48, Ile91, Asp93 and Thr184 remains open enough to allow two water molecules to insert and interact with the charged backbone atoms. The naphtol hydroxyl moiety is involved in a H-bond with the carbonyl from Asp93 (1.72 Å); the phenol ring is kept buried by hydrophobic interactions with Met98, Leu56 and Lys58, while the phenol oxygen atom is interacting with Thr184 via a hydrogen bond.

The sulphonamide linker is directly hydrogen-bonded to Asp54 (1.60 Å) and Lys112 (1.87 Å). Finally, the di-chloro substituted benzene ring does not seem to interact with any of the active site residues, and points to the solvent-exposed side of the cavity. Nevertheless, its position suggests an intramolecular conformer stabilization via a hydrophobic interaction with both naphtol and phenol ring. Its position appears to be rotated with respect to the crystallized ligand, but globally the obtained model well reproduces the reported conformation (RMSD = 1.570).

The use of high throughput screening of a library of 50,000 compounds recently led to the discovery of 3,4-diarylpyrazole Hsp90 inhibitors, which have been used as a template for further chemical modifications [41]. The crystallographic structure of a pyrazole derivative bound to Hsp90 showed that the pyrazole nitrogen atoms form a network of hydrogen bonds with the active site amino acids, together with water molecules lying on the base of the pocket. Hydrophobic interactions are also involved, including those residues which are located on the perimeter of the cavity.

Our model (Fig. 11a) revealed a good degree of similarity with the ATP binding mode template, and reproduces the binding conformation of the crystallized ligand, as confirmed by the low value of RMSD (1.045). Thus, the resorcinol moiety is positioned in the active site region originally occupied by the adenine ring, and forms two H-bonds: one directly with Asp93 (1.93 Å) and one with Ser52 (water mediated). The chlorine substituent on resorcinol points directly towards the hydrophobic cavity formed by Thr109, Phe138, Leu107, and Val150. The pyrazole ring interacts with Thr184 (2.09 Å) and Gly97 (1.84 Å); the ketone moiety of the substituent in position 5 interacts with Lys58 side chain (1.67 Å), while the ethyl terminal takes van der Waals contacts with Ile96.

Further modifications on 3,4-diarylpyrazole scaffold allowed the identification [26] of isoxazole derivatives with a higher than 20-fold increase in their ability to inhibit cancer cell proliferation compared with that of previously investigated diarylpyrazole compounds. The IFD-derived binding mode of this class of compounds (Fig. 11b) allowed us to appreciate that the overall conformation is identical to that found in the case of VER49009, with the resorcinol ring deeply buried into the pocket, corresponding to the region occupied by adenine in ATP. The network of direct and water-mediated H-bonds also demonstrates an analogous binding mode: the two resorcinol hydroxyl groups are interacting through H-bonds with Asp93 (1.85 Å) and Ser52 (through a water molecule), while the isoxazole nitrogen interacts with Gly97 backbone NH (2.98 Å). Moreover, the isoxazole 3-amide substituent contacts the backbone oxygen atom of the same residue (1.85 Å), while the amide carbonyl gives an additional interaction

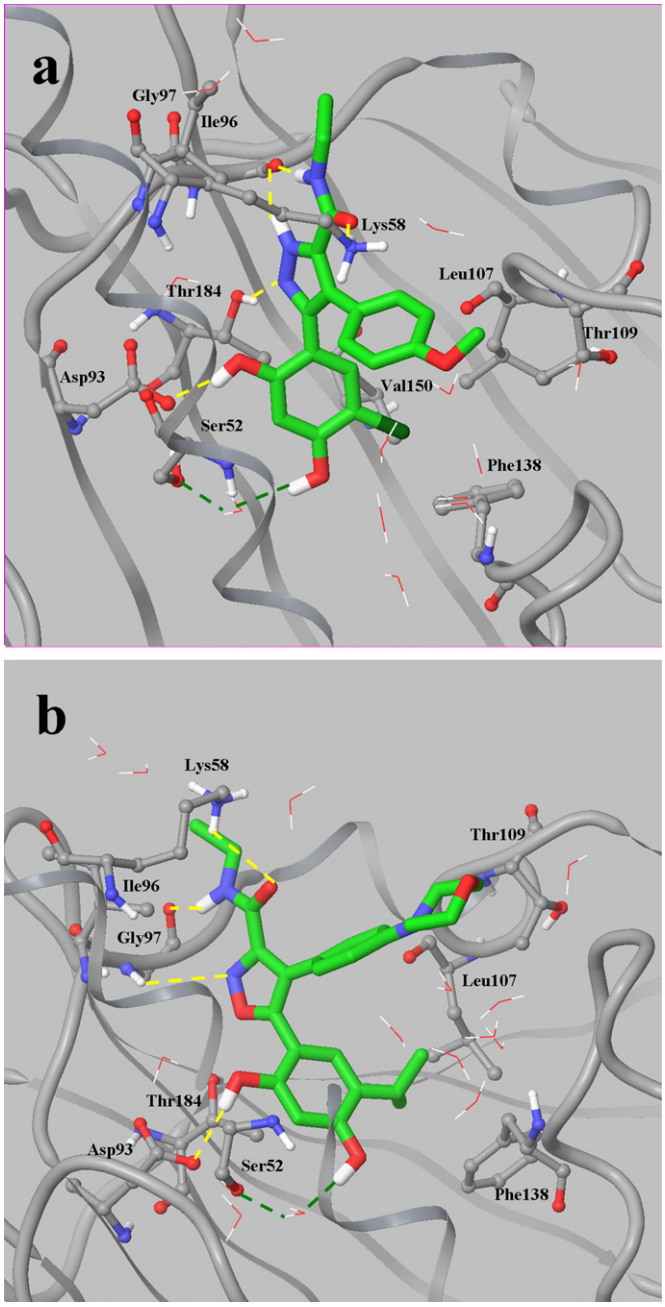

Fig. 11. Binding modes of VER49009 and isoxazole 33.

with Lys58 δ-NH_2 through a water molecule. The conformation obtained is very similar to the crystallized one (RMSD = 0.951), with little differences in the orientation of morpholin ring.

An overall view of the results obtained, in terms of molecular interactions, is given in Fig. 12 and Table 2. The alignment of the sequences of Hsp90 proteins used in this study showed a high degree of overlap, and the sequence corresponding to the active site residues is highly conserved among human (1YET, 2VCI, 2BZ5, 2BSM and 1UYF) and yeast (1AM1 and 1BGQ) sequences. Thus, a common binding cavity can be indicated: this interacts with the inhibitors through a conserved series of hydrophobic contacts (Leu48, Lys58, Met98, Thr109, Val136, Phe138, Val150 and Val186) and through direct H-bonds with Asp51, Asp54, Lys58, Asp93, Gly97, Lys112, Phe139, and Thr184.

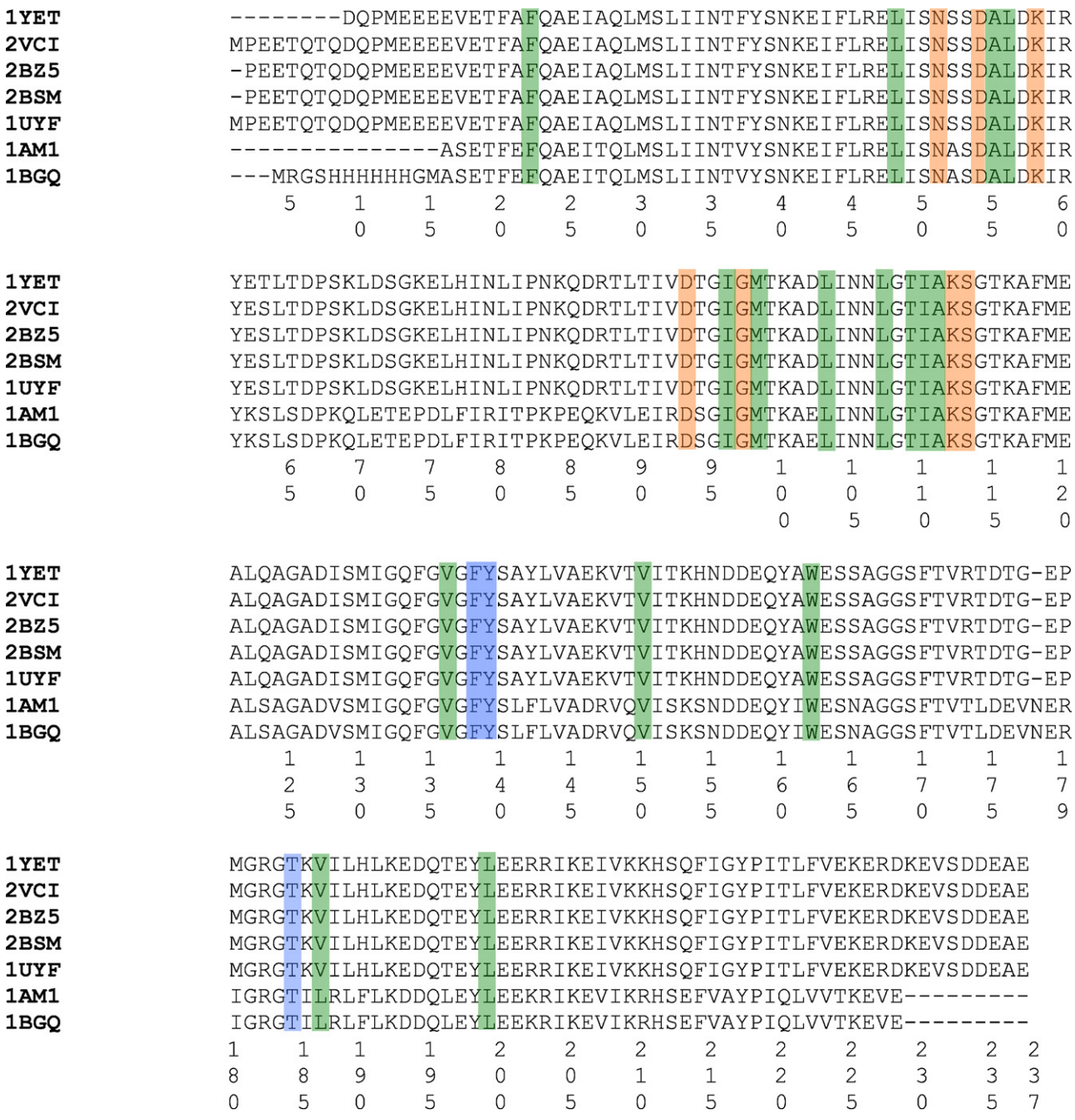

Fig. 12. Sequence alignment of the Hsp90 proteins involved in this study; orange: residues accounting for direct H-bonds; green: residues giving hydrophobic contacts; blue: residues giving both H-bonds and hydrophobic contacts (see Table 2).

The examination of the conformations obtained through the use of IFD (Fig. 13) showed that by means this technique it is possible to successfully reproduce experimental binding modes for each ligand-macromolecule complex. The RMSD values are good and substantially confirm the interactions observed in the crystal structures; the only discrepancies obtained in the case of the ATP complex can be understood considering the incomplete ligand structure of the original crystals. However, the effort to reproduce the ADP binding mode was successful (see Supplementary Material), indicating that the overall conformation of the receptor is more suitable for ADP binding than ATP; nevertheless, the use of IFD provided a binding conformation for ATP reproducing the interactions with all the Hsp90 active site residues reported to be involved in binding interactions.

Many conserved water molecules are included in each complex, and their degree of mobility is influenced by the hydrophobic surface complementarity between the inhibitor and the binding pocket pavement. Moreover, the motion of the residues placed towards the entry of the active site can accommodate relatively large hydrophobic substituents, such as halogen or methoxy-substituted phenyls, by forming a channel in which one or two water molecules can find place.

Table 2
Summary of the interacting residues in HSP90-inhibitor complexes; Residues in bracket correspond to the human homologues of yeast sequence.

Hsp90 Complexes							
ATP	Geldanamicyn	17-DMAG	Radicicol	Purines	Naphtols	Pyrazoles	Isoxazoles
Hydrophobic contacts							
Met84 (Met98)	Leu48	Ala55	Met84 (Met98)	Phe22	Leu48	Lys58	Lys58
Leu173 (Val186)	Met98	Lys58	Lys98 (Lys112)	Leu107	Leu56	Leu107	Leu107
Phe124 (Phe138)	Leu107	Ile96	Phe124 (Phe138)	Ile110	Lys58	Thr109	Thr109
	Phe138	Met98	Val136 (Val150)	Ala111	Met98	Phe138	Phe138
	Val150	Leu107	Thr171 (Thr184)	Val136	Leu107	Val150	Val150
	Val186	Phe139	Leu173 (Val186)	Phe138	Phe138		
		Val186		Thr139	Val150		
		Leu197		Trp162	Val186		
Direct H-bonds							
Lys44 (Lys58)	Asp51	Asn51	Lys44 (Lys58)	Asp93	Asp54	Asp93	Asp93
Asp79 (Asp93)	Lys58	Asp54	Asp79 (Asp93)		Thr184	Gly97	Gly97
Gly83 (Gly97)	Asp93	Lys58			Asp93	Thr184	Lys52
Lys98 (Lys112)	Lys112	Lys112			Lys112		
Ser99 (Ser113)	Phe139	Phe139					
Thr171 (Thr184)							

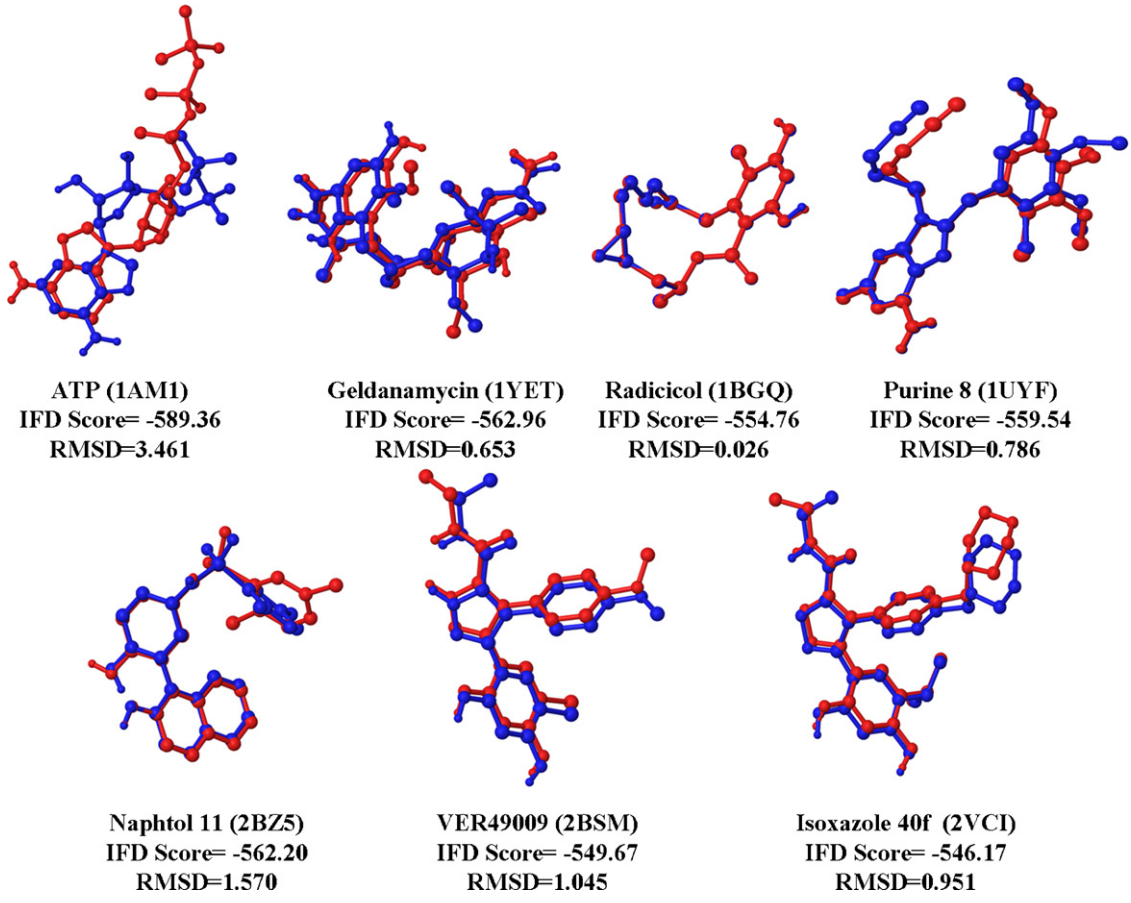

Fig. 13. RMSD superposition between the ligand conformations from the crystal structure (blue) and the pose conformation obtained by induced fit docking (red).

4. Conclusions

The availability of NMR and X-ray crystallographic structures of Hsp90/inhibitor complexes represents an enormous advantage in the fields of structural biology and medicinal chemistry. Nevertheless, the new computational tools can be successfully employed for the verification of the interactions emerged from crystal structures, because they combine conformational search procedures with a scoring function. The main goal of these procedures is generating a structure of the complex for ligands known to be active but unable to be docked in an existing structure. Moreover, the methodology can fix the artefacts which may occur during the crystallization process (i.e. crystal packing), allowing to well reproduce the experimental binding mode.

In this work we showed how the induced fit docking approach to different Hsp90/inhibitor complexes can be successfully used in order to validate existing structural models. Moreover, the use of a molecular docking algorithm coupled with a molecular dynamics

protocol, applied on the active site side chains, allowed us to simulate the dynamic behavior of the active site, which is able to change its shape in order to dock differently shaped ligand. Nevertheless, the side chain flexibility allows these residues to interact with some common moieties on each inhibitor, and also contributes to build and maintain a tight network of water molecules which complements the binding pattern of each compound. The feasibility of a rapid and affordable method for the evaluation of ligand/receptor interactions has deep implications in the drug design phase, since it allows to study the molecular mechanism of a drug candidate even prior to its synthesis. Our results represent a broad overview of the possible interactions characterizing all the Hsp90 inhibitor classes discovered to date, together with a characterization of the receptor active site in terms of shape or electronic mapping, and can be very helpful in planning new synthetic efforts devoted to the structural modifications of actual derivatives.

Appendix A. Supplementary data

Supplementary data associated with this article can be found, in the online version, at doi:10.1016/j.jmgm.2008.11.004.

References

[1] P.K. Srivastava, R.G. Maki, Stress-induced proteins in immune response to cancer, Curr. Top. Microbiol. Immunol. 167 (1991) 109–123.
[2] D.R. Ciocca, S.A.W. Fuqua, S. Lock-Lim, D.O. Toft, W.J. Welch, W.L. McGuire, Response of human breast cancer cells to heat shock and chemotherapeutic drugs, Cancer Res. 52 (1992) 3648–3654.
[3] Y. Xu, S. Lindquist, Heat-shock protein hsp90 governs the activity of pp60v-src kinase, Proc. Natl. Acad. Sci. U.S.A. 90 (1993) 7074–7078.
[4] E. Minet, D. Mottet, G. Michel, I. Roland, M. Raes, J. Remacle, C. Michiels, Hypoxia-induced activation of HIF-1: role of HIF-1alpha-Hsp90 interaction, FEBS Lett. 460 (1999) 251–256.
[5] M. Ferrarini, S. Heltai, M.R. Zocchi, C. Rugarli, Unusual expression and localization of heat shock proteins in human tumor cells, Int. J. Cancer 51 (1992) 613–619.
[6] L. Neckers, Hsp90 inhibitors as novel cancer chemotherapeutic agents, Trends Mol. Med. 8 (2002) S55–S61.
[7] J.S. Isaacs, W. Xu, L. Neckers, Heat shock protein 90 as a molecular target for cancer therapeutics, Cancer Cell 3 (2003) 213–217.
[8] T. Scheibel, J. Buchner, The Hsp90 complex—a super-chaperone machine as a novel drug target, Biochem. Pharmacol. 56 (1998) 675–682.
[9] M.P. Hernandez, W.P. Sullivan, D.O. Toft, The assembly and intermolecular properties of the hsp70–Hop–hsp90 molecular chaperone complex, J. Biol. Chem. 277 (2002) 38294–38304.
[10] C. DeBoer, P.A. Meulman, R.J. Wnuk, D.H. Peterson, Geldanamycin, a new antibiotic, J. Antibiot. 23 (1970) 442–447.
[11] J.G. Supko, R.L. Hickman, M.R. Grever, L. Malspeis, Preclinical pharmacologic evaluation of geldanamycin as an antitumor agent, Cancer Chemother. Pharmacol. 36 (1997) 305–315.
[12] M.J. Egorin, T.F. Lagattuta, D.R. Hamburger, J.M. Covey, K.D. White, S.M. Musser, J.L. Eiseman, Pharmacokinetics, tissue distribution, and metabolism of 17-(dimethylaminoethylamino)-17-demethoxygeldanamycin (NSC 707545) in CD2F1 mice and Fischer 344 rats, Cancer Chemother. Pharmacol. 49 (2002) 7–19.
[13] http://clinicaltrials.gov/ct2/show/NCT00506805.
[14] B.W. Dymock, M.J. Drysdale, E. McDonald, P. Workman, Inhibitors of HSP90 and other chaperones for the treatment of cancer, Expert Opin. Ther. Pat. 14 (2004) 837–847.
[15] L. Neckers, K. Neckers, Heat-shock protein 90 inhibitors as novel cancer chemotherapeutics—an update, Expert Opin. Emerging Drugs 10 (2005) 137–149.
[16] http://www.pdb.org.
[17] W. Scherman, T. Day, M.P. Jacobson, R.A. Friesner, R. Farid, Novel procedure for modeling ligand/receptor induced fit effects, J. Med. Chem. 49 (2006) 534–553.
[18] T. Liu, Y. Lin, X. Wen, R.N. Jorrisen, M.K. Gilson, BindingDB: a web-accessible database of experimentally determined protein-ligand binding affinities, Nucleic Acids Res. 35 (2007) D198–D201.
[19] C.E. Stebbins, A.A. Russo, C. Schneider, N. Rosen, F.U. Hartl, N.P. Pavletich, Crystal structure of an Hsp90-geldanamycin complex: targeting of a protein chaperone by an antitumor agent, Cell 89 (1997) 239–250.
[20] S.M. Roe, C. Prodromou, R. O'Brien, J.E. Ladbury, P.W. Piper, L.H. Pearl, Structural basis for inhibition of the Hsp90 molecular chaperone by the antitumor antibiotics radicicol and geldanamycin, J. Med. Chem. 42 (1999) 260–266.
[21] X. Barril, P. Brough, M. Drysdale, R.E. Hubbard, A. Massey, A. Surgenor, L. Wright, Structure-based discovery of a new class of Hsp90 inhibitors, Bioorg. Med. Chem. Lett. 15 (2005) 5187–5191.
[22] B.W. Dymock, X. Barril, P.A. Brough, J.E. Cansfield, A. Massey, E. McDonald, R.E. Hubbard, A. Surgenor, S.D. Roughley, P. Webb, P. Work man, L. Wright, M.J. Drysdale, Novel, potent small-molecule inhibitors of the molecular chaperone Hsp90 discovered through structure-based design, J. Med. Chem. 48 (2005) 4212–4215.
[23] K.M.J. Cheung, T.P. Mattews, K. James, M.G. Rowlands, K.J. Boxall, S.Y. Sharp, A. Maloney, S.M. Roe, C. Prodromou, L.H. Pearl, G.W. Aherne, E. McDonald, P. Workman, The identification, synthesis, protein crystal structure and in vitro biochemical evaluation of a new 3,4-diarylpyrazole class of Hsp90 inhibitors, Bioorg. Med. Chem. Lett. 15 (2005) 3338–3343.
[24] L. Wright, X. Barril, B. Dymock, L. Sheridan, A. Surgenor, M. Beswich, M. Drysdale, A. Collier, A. Massey, N. Davies, A. Fink, C. Fromont, W. Aherne, K. Boxall, S. Sharp, P. Workman, R.E. Hubbard, Structure-activity relationships in purine-based inhibitor binding to HSP90 isoforms, Chem. Biol. 11 (2004) 775–785.
[25] P.A. Brough, W. Aherne, X. Barril, J. Borgognoni, K. Boxall, J.E. Cansfield, K.M.J. Cheung, I. Collins, N.G.M. Davies, M.J. Drysdale, B. Dymock, S.A. Eccles, H. Finch, A. Fink, A. Hayes, R. Howes, R.E. Hubbard, K. James, A.M. Jordan, A. Lockie, V. Martins, A. Massey, T.P. Mattews, E. McDonald, C.J. Northfield, L.H. Pearl, C. Prodromou, S. Ray, F.I. Raynaud, S.D. Roughley, S.Y. Sharp, A. Surgenor, D.L. Walmsey, P. Webb, M. Wood, P. Workman, L. Wright, 4,5-Diarylisoxazole Hsp90 chaperone inhibitors: potential therapeutic agents for the treatment of cancer, J. Med. Chem. 51 (2008) 196–218.
[26] C. Prodromou, S.M. Roe, R. O'Brien, J.E. Ladbury, P.W. Piper, L.H. Pearl, Identification and structural characterization of the ATP/ADP-binding site in the Hsp90 molecular chaperone, Cell 90 (1997) 65–75.
[27] SiteMap, version 2.1, Scrödinger, LLC, New York, NY, 2007.
[28] I. Halperin, B. Ma, H. Wolfson, R. Nussinov, Principles of docking: an overview of search algorithms and a guide to scoring functions, Proteins 47 (2002) 409.
[29] S.P. Sousa, P.A. Fernandes, M.J. Ramos, Protein-ligand docking: current status and future challenges, Proteins 65 (2006) 15.
[30] J. Janin, J. Cherfils, Protein docking algorithms: Simulating molecular recognition, Curr. Opin. Struct. Biol. 3 (1993) 265.
[31] D.B. Kokh, W. Wenzel, Flexible side chain models improve enrichment rates in silico screening, J. Mol. Med. 51 (2008) 5919.
[32] R.M.A. Knegtel, I.D. Kuntz, C.M. Oshiro, Molecular docking to ensembles of protein structures, J. Mol. Biol. 266 (1997) 424.
[33] E.A. Sudbeck, C. Mao, T.K. Venkatachalam, L. Thuel-Ahlgren, F.M. Uckum, Structure-based design of novel dihydroalkoxybenzyloxopyrimidine derivatives as potent nonnucleoside inhibitors of the human immunodeficiency virus reverse transcriptase, Antimicrob. Agents Chemother. 42 (1998) 3225.
[34] G.M. Morris, D.S. Goodsell, R.S. Halliday, R. Huey, W.E. Hartl, R.K. Belew, A.J. Olson, Automated docking using a Lamarckian genetic algorithm and an empirical binding free energy function, J. Comput. Chem. 19 (1998) 1639.
[35] Y.S. Pak, S. Wang, Application of a molecular dynamics simulation method with a generalized effective potential to the flexible molecular docking problems, J. Phys. Chem. B 104 (2000) 354.
[36] Glide, version 4.5, Scrödinger, LLC, New York, NY, 2005.
[37] Prime, version 1.6, Scrödinger, LLC, New York, NY, 2005.
[38] S.C. Lovell, I.W. Davis, W.B. Arendall, P.I.W. De Bakker, J.M. Word, M.G. Prisant, J.S. Richardson, D.C. Richardson, Structure validation by C-alpha geometry: phi, psi, and C-beta deviation, Prot. Struct. Funct. Gen. 50 (2002) 437–450.
[39] G. Chiosis, M.N. Timaul, B. Lucas, P.N. Munster, F.F. Zheng, L. Sepp-Lorenzino, N. Rosen, A small molecule designed to bind to the adenine nucleotide pocket of Hsp90 causes Her2 degradation and the growth arrest and differentiation of breast cancer cells, Chem. Biol. 8 (2001) 289–299.
[40] X. Barril, R.E. Hubbard, S.D. Morley, Virtual screening in structure-based drug discovery, Mini Rev. Med. Chem. 4 (2004) 779–791.
[41] P.A. Brough, X. Barril, M. Beswick, B.W. Dymock, M.J. Drysdale, L. Wright, K. Grant, A. Massey, A. Surgenor, P. Workman, 3-(5-Chloro-2, 4-dihydroxyphenyl)-pyrazole-4-carboxamides as inhibitors of the Hsp90 molecular chaperone, Bioorg. Med. Chem. Lett. 15 (2005) 5197–5201.